Vol. 68: 137–149, 2016
doi: 10.3354/cr01340

CLIMATE RESEARCH
Clim Res

Published May 4

Contribution to CR Special 32 'CLARIS-La Plata Basin: climate variability and uncertainties'

Köppen–Trewartha classification used to assess climate changes simulated by a regional climate model ensemble over South America

C. Gallardo[1,*], V. Gil[2], C. Tejeda[1], E. Sánchez[1], M. A. Gaertner[1]

[1]University of Castilla-La Mancha, Faculty of Environmental Sciences and Biochemistry, Avda. de Carlos III s/n, 45071 Toledo, Spain

[2]University of Lisbon, Instituto Dom Luiz (IDL), Faculty of Sciences, Campo Grande, 1749-016 Lisbon, Portugal

ABSTRACT: The Köppen–Trewartha climate classification was applied to regional climate model (RCM) simulations obtained in the frame of the CLARIS-LPB EU project to assess the ability of RCMs to reproduce the climate in South America and to inquire into the extent, magnitude and trend of the expected climate change in this region. Three sets of simulations were analysed: hindcast simulations, in which RCMs were driven by ERA-Interim reanalysis; historical simulations, where RCMs were nested in general circulation models (GCMs) for the period 1961–1990; and scenario simulations, where RCMs were driven by the SRES A1B scenario simulations performed by GCMs for 2 periods, 2011–2040 and 2071–2100. The co-occurrence matrices used allow a grid-to-grid comparison of climates derived from both hindcast simulations and observations. They also allow the comparison of simulations for 2 different periods. The climates of almost 70% of the surface of the domain were correctly described by the ensemble of the regional model hindcast simulations, with the main difference with observations being the location of the line between the 2 tropical climates. The historical simulations reached an agreement of 60.9% with the observations. It is projected that 12% of the area of South America will be affected by significant climate changes for 2011–2040 and around 27% for 2071–2100. Transitions to wetter climates are mainly found in the northern half of Argentina. Transitions to drier climates are principally projected over Brazil. Very strong climate changes are expected in some zones of the Andes mountain range. The climate that appears to be involved in a greater number of future transitions is the subtropical humid climate.

KEY WORDS: Climate change · Regional climate · South America · Köppen–Trewartha classification

1. INTRODUCTION

The use of a climate classification like that of Köppen–Trewartha (Trewartha & Horn 1980) (hereafter KT) allows for an integrated study of 2 variables important for climate, such as precipitation and 2 m temperature (hereafter t2m). Additionally, since there is a strong relationship between the KT climate type at a location and its potential vegetation, the application of this methodology allows a preliminary assessment of the significance of the effects of climate change on ecosystems.

The Köppen classification has been satisfactorily applied to the output of regional climate models (RCMs) or general circulation models (GCMs) in several zones of the Earth, as can be seen in Shi et al. (2012) and Baker et al. (2010) for China, Gao & Giorgi (2008) for the Mediterranean region, Roderfeld et al. (2008) for the Barents Sea region or Gallardo et al. (2013) for the entire European region. Nevertheless,

*Corresponding author: clemente.gallardo@uclm.es

a similar study has not been addressed until now for a region as large and climatologically diverse as South America (hereafter SA). This work attempts to fill this gap. This has been possible because, in the framework of the European project CLARIS-LPB (A Europe-South America Network for Climate Change Assessment and Impact Studies in La Plata Basin), a relatively recent climatic ensemble of RCMs over SA has been completed.

SA comprises a region with a very complex terrain and a wide variety of vegetation. These factors imply that there are numerous small-scale processes in the region which together with other synoptic and large-scale mechanisms, such as the South American monsoon system or the South American low-level jet (e.g. Vera et al. 2006a,b), among others, give rise to a huge variety of climates. In this region, there are practically all possible climates, from alpine to desert, temperate or jungle (Garreaud et al. 2009). These characteristics make KT particularly suitable for the study of climate in SA as compared to other regions with more homogeneous climate.

The spatial resolution of GCMs (in this study, 3.75° × 2.5° for HadCM3 and IPSL, and approximately 1.9° × 1.9° for EC5OM) cannot account for fine-scale processes that are important in many zones of SA. RCMs usually work with a spatial resolution between 10 and 50 km, which allows them to provide more detail in topography, distribution of vegetation and coastlines than GCMs. Many studies (e.g. Dimitrijevic & Laprise 2005, Antic et al. 2006, Feser 2006, Christensen et al. 2007, Laprise 2008) have shown that because of this greater spatial detail, RCMs have the ability to effectively simulate small-scale climatic phenomena, although the reanalysis or GCMs in which they are nested do not provide them with information about these fine-scale processes through the lateral boundary values. This makes RCMs a good complement to GCMs in climate studies, because they introduce added value by considering small-scale climatic features.

Although the RCMs of CLARIS-LPB use a resolution of about 50 km, which may limit their ability to describe some climatic features of SA, it seems reasonable to expect an improvement in the representation of climate when compared with GCM results. Recently, Solman et al. (2013) examined the ability of several RCM simulations (just the ones nested in the ERA-Interim reanalysis among those used for this work) to reproduce the climatic features of SA, and found that the ensemble of RCMs accurately simulates the seasonal averages, annual cycles and frequency distribution of the monthly averages for different representative subregions of the continent for precipitation and t2m. However, the multi-model ensemble showed larger biases and uncertainties in tropical regions than in the subtropics. In addition, some important problems representing seasonal averages and annual cycles were detected, such as winter precipitation in the Uruguay subbasin.

In this work, we took advantage of the features of KT indicated above and applied it to the results of the RCM simulations of the CLARIS-LPB project, driven by both reanalysis and GCMs. This allows for an assessment of the ability of RCMs to reproduce the climate of SA and also assesses the extent and magnitude of the expected climate change. In addition, it explores the trend of change by detailing which climates would replace those that recede in the region.

2. METHODS

For this study, KT subtypes have been calculated for the simulations of 7 RCMs included in the CLARIS-LPB project (Table 1). These simulations followed the CORDEX phase I protocol (Giorgi et al. 2009), where an effort to coordinate RCM simulations over selected subregions of the world is proposed. All models covered the region defined between latitudes 60° S and 15° N and longitudes 90° W and 20° W, that is, all of SA (Fig. 1). The horizontal resolution used by the models was about 50 km.

Three sets of simulations were analysed. The first simulation consisted of hindcast simulations to first inspect the capability of the RCMs to describe the main features of the climate of the region. In these hindcast simulations, the initial and boundary conditions were taken from the ERA-Interim reanalysis dataset (Simmons et al. 2007, Dee et al. 2011) for the period 1990–2008. More details about the models and validation of the ensemble of RCMs can be found in Solman et al. (2013).

The second set of simulations (scenario simulations) covered 2 future climate periods (2011–2040 and 2071–2100) to study changes due to the increase in greenhouse gases. Ten climate simulations from 6 RCMs were driven by the SRES A1B scenario (Nakićenović et al. 2000) simulations performed by 3 different GCMs, as shown in Table 1. In the third set of simulations (historical simulations), 10 climate simulations were produced by nesting the 6 RCMs in the 3 GCMs in the same manner as in the scenario simulations but for the period 1961–1990. These simulations serve as a reference for the scenario simulations to analyse the projected climate change for the 21st

Table 1. Basic information of the participating models. RCM: regional climate model; GCM: general circulation model; ND: no data available for the MM5 model for the historical and scenario simulations

RCM models	Responsible institution/model version	Driving GCM	Basic references for RCMs
RCA	Rossby Centre, Swedish Meteorological and Hydrological Institute/RCA3.5	EC5OMr3[a], EC5OMr2, EC5OMr1	Samuelsson et al. (2010, 2011)
REMO	Max Planck Institute for Meteorology, Hamburg/REMO2009	EC5OMr1	Jacob et al. (2001, 2012)
PROMES	Grupo MOMAC, Area Física de la Tierra, Facultad Ciencias Medio Ambiente, Universidad Castilla-La Mancha/PROMES2.4	HadCM3	Sánchez et al. (2007), Domínguez et al. (2010)
REGCM3 v3	GrEC-USP, Departamento de Ciencias Atmosféricas, Universidade de Sao Paulo, Brasil/ RegCM3	EC5OMr1, HadCM3	Pal et al. (2007), da Rocha et al. (2009)
MM5	Centro de Investigaciones del Mar y la Atmósfera CIMA/MM5V3.7	ND	Grell et al. (1994), Solman & Pessacg (2012)
LMDZ	IPSL, Institute Pierre-Simon Laplace/LMDZ4	EC5OMr1, IPSL	Hourdin et al. (2006), Li (1999)
ETA	Instituto Nacional de Pesquisas Espaciais, INPE/ETA Climate change V1.0	HadCM3	Pesquero et al. (2010), Chou et al. (2012)

[a]ECHAM5 is the atmospheric component of EC5OM; the results of 3 different versions of this GCM were used in the present work

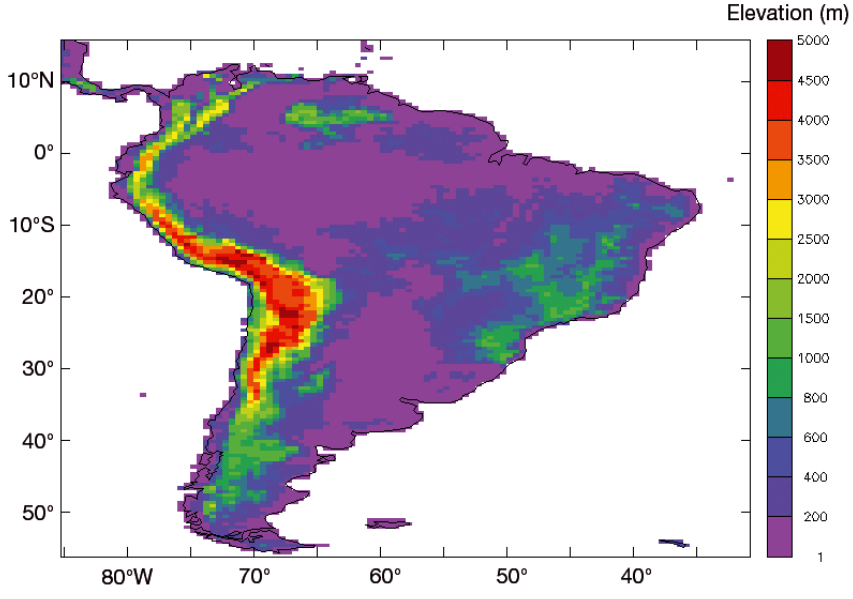

Fig. 1. Model domain and topography

century. Most of the RCMs in the CLARIS-LPB project were only nested in GCMs for three 30 yr periods (1961–1990, 2011–2040 and 2071–2100); therefore, in this study, only these 3 periods can be used. A preliminary look at this climate ensemble experiment has been shown in Sánchez et al. (2011, 2015) and Samuelsson et al. (2013).

In this work, the KT climate classification (Table 2), which is an improvement on the original Köppen classification, was used. KT does not need daily data but instead calculates its climate types from monthly climatological data; this allows it to be used on virtually the entire surface of the Earth. KT was applied over all of SA (Fig. 1) to monthly mean t2m and precipitation data derived from the 7 hindcast simulations, 10 scenario simulations and 10 historical simulations described above. Only land points were considered, as the observational databases combining t2m and precipitation were only available on those points. As shown in Solman et al. (2013), only 2 observational gridded datasets which include both temperature and precipitation simultaneously are available over the region. They show similar values for temperature on both monthly and seasonal scales (Mitchell & Jones 2005, Matsuura & Willmott 2009). When considering just precipitation, these datasets show important differences in some zones of SA (Solman et al. 2013). We used one of these datasets, the Climate Research Unit (CRU, University of East Anglia) observational database, which has been widely used to validate RCM simulations all over the world. The resolution of the CRU version used is 0.5°, which is equal or similar to that of the analysed

Table 2. Köppen–Trewartha climate classification (Trewartha & Horn 1980). P: precipitation (cm)

Climate type	Description	Classification criteria
Ar	Tropical humid	All months >18°C and <3 dry months[a]
Aw	Tropical wet-dry	All months >18°C and ≥3 dry months
BW	Dry arid	$P \leq 0.5A$[b]
BS	Dry semiarid	$0.5A < P \leq A$
Cs	Subtropical summer-dry	8–12 mo ≥10°C, annual rainfall <89 cm and dry summer[c]
Cw	Subtropical summer wet	8–12 mo ≥10°C, dry winter[d]
Cr	Subtropical humid	8–12 mo ≥10°C, with no dry season
Do	Temperate oceanic	4–7 mo ≥10°C and coldest month >0°C
Dc	Temperate continental	4–7 mo ≥10°C and coldest month <0°C
Eo	Subarctic oceanic	Up to 3 mo ≥10°C and t2m of the coldest month >–10°C
Ec	Subarctic continental	Up to 3 mo ≥10°C and t2m of the coldest month ≤–10°C
Ft	Tundra	All months <10°C, but at least 1 mo ≥0°C
Fi	Ice cap	All months <0°C

[a]Dry month: <6 cm monthly precipitation
[b]$A = 2.3 \cdot T - 0.64 \cdot Pw + 41$, where T is the mean annual 2 m temperature (t2m, in °C), and Pw is the percentage of annual precipitation occurring in the coolest 6 mo
[c]Dry summer: driest summer month <3 cm precipitation and less than one-third of the amount in the wettest winter month
[d]Dry winter: precipitation in the wettest summer month >10 times that of the driest winter month

RCMs. The project CLARIS-LPB provided the data for all of its simulations interpolated to the 0.5° CRU mesh, which facilitated the comparison between observations and model results. The KT climates were also calculated for the ensemble of models for hindcast, historical and scenario simulations. To build the ensemble, we calculated the average of the monthly climatological values of all available models in each case for t2m and precipitation; the KT subtypes of the ensemble were calculated from those averaged fields.

The results from the output of each hindcast simulation were compared with KT subtypes obtained from the CRU observational dataset to check the capacity of the RCMs to correctly describe the main observed climatic types and characteristics of the region. For the historical simulations, KT climates were calculated for the period 1961–1990 (the reference period). For each scenario, simulation KT climates were calculated for 2 time slices of 30 yr each (2011–2040 and 2071–2100). In this way, the projected evolution of climate in SA since the late 20th century to the end of the current century can be assessed. In all 3 cases (hindcast, historical and scenario simulations), KT climates were also calculated for an equally weighted ensemble of all available RCMs.

Following the methodology of Gallardo et al. (2013) and de Castro et al. (2007), a grid-to-grid comparison of the individual hindcast or historical simulations and their ensemble with the CRU database was done through the development of co-occurrence matrices. These matrices allow assessment of the level of correspondence between KT subtypes of the observed climatology and those of each simulation or the ensemble for the period (1990–2008) in which RCMs were driven by the Era-Interim reanalysis or for the period (1961–1990) in which RCMs were driven by GCMs. Similar co-occurrence matrices allow comparison of KT climates between each of the scenario simulations and the historical simulations. This enables the quantification of projected climate trends throughout the 21st century.

For a better interpretation of the co-occurrence matrices used to assess the hindcast and historical simulations, the following points should be remembered: (1) The climates (see top of Table 3) refer to those derived from the hindcast or historical simulations, whereas the climates that appear on the left side of the table refer to those derived from observations (CRU). Thus, in a row of the matrix, we can see what climates have been assigned by a model (or ensemble of models) for a given climate assigned by the observations. Likewise, in a column of the matrix, we can see what climates have been assigned by the observations (CRU) for a given climate assigned by a model (or ensemble of models). (2) The main diagonal of each matrix indicates the area (in thousands of square kilometers) where the KT subtype according to the CRU database matches that generated from a single simulation or the ensemble of models. (3) A number greater than zero outside of the main diagonal of the matrix indicates a lack of coincidence. A larger separation from the diagonal indicates larger differences between the observations and the simulation or the ensemble. (4) Nonzero elements below the main diagonal indicate that the simulation or the ensemble is warmer or drier than the CRU. (5) Conversely, nonzero elements above the main diagonal indicate that the

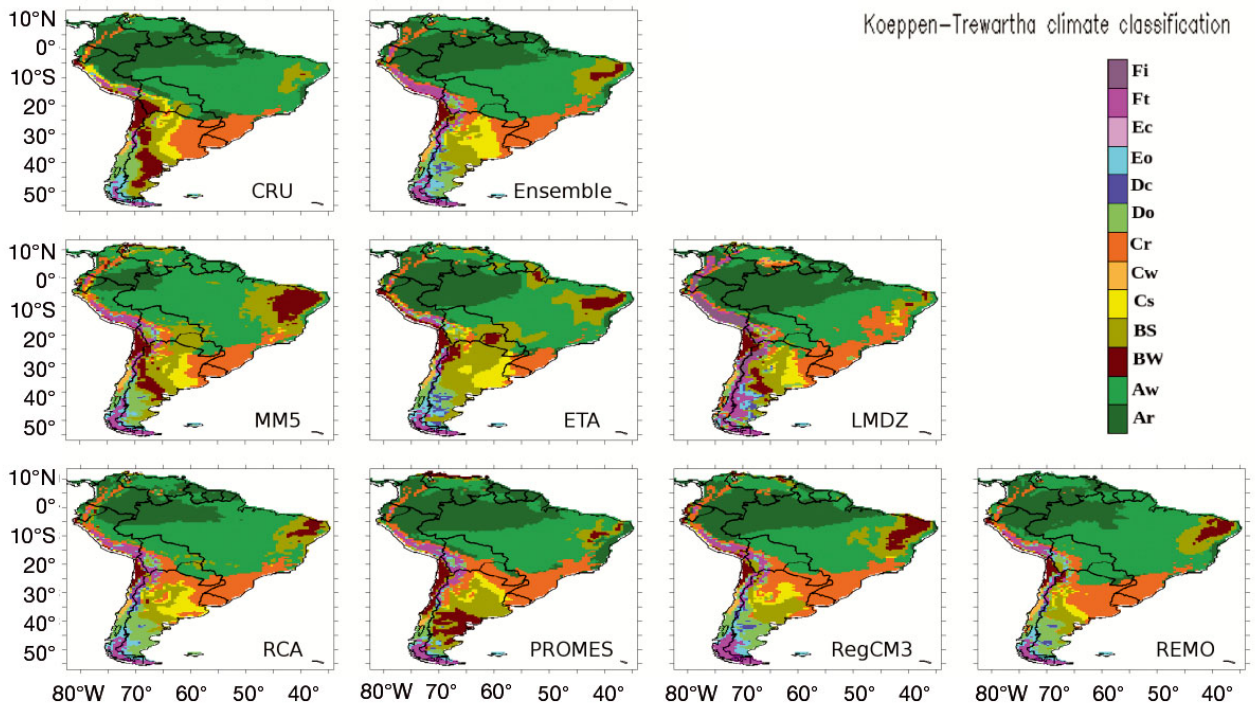

Fig. 2. Spatial distribution of Köppen–Trewartha climate subtypes (see Table 2) over South America according to observations (Climate Research Unit [CRU] dataset), 7 regional climate model (RCM) hindcast simulations forced with ERA-Interim reanalysis and their ensemble for the period 1990–2008

simulation or the ensemble is cooler or wetter than the CRU.

A second type of co-occurrence matrix is used in this work to compare the future climates projected by scenario simulations (or their ensembles) and the climates derived from historical simulations (or its ensemble) for the reference period (1961–1990). Essentially, these co-occurrence matrices are the same as those described previously. They differ only in that the climates at the top of the table refer to scenario simulations (or their ensembles), and the climates on the left side of the table refer to the reference period (1961–1990) of the historical simulations (or its ensemble).

Everything for the first type of co-occurrence matrix applies to this second type, except 'CRU' or 'observations' is changed to 'historical simulations or its ensemble' and 'simulation' is changed to 'scenario simulation'. The first type of co-occurrence matrix is used in Sections 3.1 and 3.2 of this work, and the second type is used in Section 3.3. In the 3 co-occurrence matrices shown in this work, data derived from the models were not directly used; instead, data from ensembles of models were utilized. The co-occurrence matrices were also constructed with data from single models, but only certain aggregated results are shown in this study.

3. RESULTS

3.1. Evaluation of hindcast simulations (1990–2008)

Fig. 2 shows KT climates for the period 1990–2008, as simulated by the 7 RCMs forced with ERA-Interim reanalysis, together with those calculated with the CRU observational gridded dataset and the ensemble average from the 7 RCM models. As complementary information, co-occurrence matrices of observations and the ensemble of models (Table 3) or each of the 7 individual models (not shown) were built.

The domain considered in this work covers about 17 809 × 10^3 km^2 of land surface. However, the ensemble co-occurrence matrix (Table 3) shows a surface of 12 393 × 10^3 km^2 along the main diagonal. This means that in almost 70 % of the surface of SA, the KT climate from the ensemble coincides with the KT climate from observations. When looking at individual models (Table 4), these value range from 48 to 67 %, although 6 of 7 models are above 59 %.

Tropical humid (*Ar*) and tropical wet-dry (*Aw*) climates represent almost two-thirds of the surface of SA (see the map derived from observations in Fig. 2). These climates are reasonably well represented in simulations, since the ensemble of RCMs coincides with observations over around 79 % of the surface of

Table 3. Co-occurrence matrix between model ensemble (top of the table) and Climate Research Unit dataset (left) for the reference period (1961–1990). Values are in thousands of square kilometers

	BW	*BS*	*Ar*	*Cs*	*Cw*	*Aw*	*Cr*	*Do*	*Dc*	*Eo*	*Ec*	*Ft*	*Fi*
BW	186.5	351.7	0	29.1	0	6.1	5.6	159.8	20.2	31.6	0	79.8	0
BS	133	683.7	3	90.1	0	194.2	116.8	182.1	19	40.5	0	132.6	5.5
Ar	0	0	4143	0	0	845.6	137.2	0	0	0	0	0	0
Cs	0	112.5	0	150.9	0	0	190.3	26	0	0	0	66.9	0
Cw	0	0	0	0	53.1	0	6.1	0	0	0	0	0	0
Aw	42.9	489	685.4	8.6	0	5265	234.1	0	0	0	0	0	0
Cr	0	20.9	0	388.3	3	28.1	1364	6.1	0	3.1	0	27.7	0
Do	0	0	0	0	27.6	0	14	198	73.7	148.8	0	59.3	0
Dc	0	0	0	0	0	0	0	0	0	2.1	0	5.1	0
Eo	0	0	0	0	0	0	0	6.3	0	80.6	0	145.9	0
Ec	0	0	0	0	0	0	0	0	0	0	0	0	0
Ft	0	0	0	0	0	0	0	0	0	0	0	269	10.6
Fi	0	0	0	0	0	0	0	0	0	0	0	0	0

Table 4. Percentage of the total studied area located on the main diagonal of the co-occurrence matrices for hindcast simulations for each analysed regional climate model (RCM) and ensemble of models (second column). Difference of performance (percentage of the total area on the main diagonal of the co-occurrence matrices) between historical and hindcast simulations (historical minus hindcast) for each analysed RCM and ensemble of models (third column). The RCMs nested in more than one general circulation model (see Table 1) have a result in this third column for each nesting. ND: no data available for the MM5 model for historical and scenario simulations

RCM/Institution	Percentage in the main diagonal	Difference of performance (historical – hindcast)
MM5/CIMA	48.0	ND
ETA/INPE	59.0	+5.3
LMDZ/IPSL	58.9	−4.9/−6.1
REMO/MPI	67.1	−1.9
RCA/SMHI	64.7	−8.3/−8.9/−8.0
PROMES/UCLM	66.3	−4.1
RegCM3/USP	61.8	−7.4/−9.8
Ensemble	69.6	−8.7

tropical climates. For all of the models (except MM5, with around 46%), that percentage of coincidence is between 66 and 77%. Nevertheless, as the absolute value of such areas is quite large, small discrepancies in that percentage mean quite a large area in terms of square kilometers. The area with a *BW* arid climate around southwestern Bolivia, north of Chile and east of the Argentinean Andes, is one of the areas where models show larger differences. Four of them (RCA, REMO, REGCM3 and ETA) hardly simulate this climate type, and the other 3 (PROMES, MM5 and LMDZ) show it, but with smaller size or the wrong location. The best model (MM5) related to *BW* climate over this area is the one with the worst overall performance, being too dry over other areas (very reduced *Ar* and a very large *BW* zone in northeastern SA).

Over northeastern Argentina, the observed subtropical humid climate (*Cr*) is changed to subtropical summer-dry (*Cs*) or even semiarid (*BS*) for all models (except REMO), indicating a tendency toward simulated climates drier than the observed ones. This is probably partially related to the underestimation of seasonal precipitation obtained by the models over that region and time period (Solman et al. 2013). The ensemble mean usually changes *Cr* to *Cs* over that area.

Over Argentinean Patagonia, temperate oceanic (*Do*) areas close to the Andes are modelled as colder climates (temperate continental [*Dc*] and subarctic oceanic [*Eo*]) for most of the models and the ensemble. Also, *BS* observed climates are usually simulated as *Do*.

For northeastern Brazil, most of the models tend to be too dry, as already noted in Solman et al. (2013), changing *Aw* to *BS* or even *Aw* and *BS* to *BW*. At the southeastern Brazilian coast, many models (except MPI and Eta) obtain a larger *Cr* area than observations, where *Aw* should be obtained. This result could be related to the lower modelled temperatures or precipitation amounts.

The final relevant discrepancy among models and observations is related to mountainous areas. CRU shows them as *Eo* climate, but models and their ensembles associated them with *Ft* (tundra), which is a colder climate than what observations give. Even the LMDZ model is too cold when compared with other models on mountainous regions, with an *Fi* climate (ice cap). With a horizontal resolution of 50 km,

Table 5. Percentage of the total studied area located on the main diagonal of the co-occurrence matrices for each analysed general circulation model–regional climate model (GCM-RCM) pair for the period 1961–1990 of the historical simulations. The ensemble does not include the ETA model because of the lack of data in some latitudes

RCM/ Institution	GCM HadCM3	EC5OMr1	EC5OMr2	EC5OMr3	IPSL
ETA/INPE	64.3				
LMDZ/IPSL		54.0			52.8
REMO/MPI		65.2			
RCA/SMHI		56.4	55.8	56.7	
PROMES/ UCLM	62.2				
RegCM3/ USP	54.4	52.0			
Ensemble 60.9					

the orography of the RCMs may be significantly distorted over some parts of the mountain chain due to its steep structure, and this could partially explain such discrepancies. However, it is quite probable that there is a lack of reliable mountain stations used to obtain the CRU gridded database as pointed out by Rauscher et al. (2010) or Urrutia & Vuille (2009), and it could be critical for evaluating model performance over areas with steep orography.

All of these differences between models and observations explain most of the discrepancies between them. There are other differences, but they are smaller and more dispersed.

3.2. Historical simulation analysis

In Table 5, the level of coincidence between KT climates generated from CRU observations and those derived from historical simulations of different RCMs can be seen for the reference period 1961–1990. The coincidence for observed and simulated climates ranges from 52% of the total area to 65.2%. For the ensemble, the matching reaches 60.9%. The different versions of EC5OM do not seem to generate large differences in this regard, as the RCA model was nested in these 3 versions giving similar coincidence values in the 3 cases (between 55.8 and 56.7%). REMO seems to overtake the other RCMs nested in the GCM of MPI; however, LMDZ achieves similar results when nested in 2 different GCMs. It is striking that ETA gives better results when nested in HadCM3 (64.3% of coincidence) than when nested in ERA-Interim (59.0%). This can be partly explained because the historical simulation of this model is not compared to observations for gridpoints with latitude beyond 50° S due to a lack of data for this simulation. However, in general (Table 4), the RCMs do slightly worse in the historical simulation than in the hindcast simulation. On average, there are 5.4 percentage points less of coincidence. However, the results are not far from the optimal set by the hindcast simulations.

3.3. Projected climate change

In this section, 2 sets of scenario simulations are compared with the set of historical simulations (reference period 1961–1990) to assess projected climate change in the region. Co-occurrence matrices analysis (Tables 6 & 7) indicates a clear trend for future climate conditions to a displacement toward drier or warmer climates. But some changes in the opposite direction are also obtained. For the ensemble, the percentage over the total area where climates are changed to drier or warmer types is around 24% when comparing the 2071–2100 period against the reference climate (1961–1990) and 11.4% when the 2011–2040 future period is considered. The percentage of change toward wetter climates is 2.8% for 2071–2100 and just 0.5% for 2011–2040. Most of this change is related to the extension of subtropical humid climate (*Cr*) in the northern half of Argentina (Figs. 3–5).

Comparing Figs. 4 & 5 (future climate) with Fig. 3 (reference period), it can be seen that over most of the Brazil region, the ensemble indicates a reduction in wet climates (tropical humid [*Ar*] and subtropical humid [*Cr*]) due to the increase in a drier one (tropical wet-dry [*Aw*]). A displacement to warmer climates over the whole Andes chain is also obtained. Almost all of the RCMs agree when simulating both trends on their climate change projections. Nevertheless, the northern half of Argentina is shown by the ensemble to exhibit a change toward wetter climates for the 21st century, mainly due to transitions from subtropical summer-dry (*Cs*) to *Cr*. Here, just 6 out of 10 of the RCM simulations agree on such change. These results are consistent with those shown in other works such as Vera et al. (2006c) or Sánchez et al. (2015).

Fig. 6 shows the projected transfers between the different KT subtypes, where the net area changes in each given subtype are also indicated. The most remarkable result is that the subtype of climate *Aw*

Table 6. Co-occurrence matrix between the scenario ensemble of models for the period 2011–2040 (top of table) and the ensemble of historical simulations (1961–1990, left). Values are in thousands of square kilometers

	BW	*BS*	*Aw*	*Cs*	*Cw*	*Ar*	*Cr*	*Do*	*Dc*	*Eo*	*Ec*	*Ft*	*Fi*
BW	71.3	8.3	0	0	0	0	0	0	0	0	0	0	0
BS	18	187.9	0	2.6	2.8	0	2.8	0	0	0	0	0	0
Aw	0	21.2	4650.5	0	0	6.1	0	0	0	0	0	0	0
Cs	0	5.3	0	350.5	0	0	39.6	0	0	0	0	0	0
Cw	0	0	0	0	64.6	18.4	0	0	0	0	0	0	0
Ar	0	0	789.4	0	0	6186.9	0	0	0	0	0	0	0
Cr	0	21.9	310.5	28	23.4	210.9	2603.9	0	0	0	0	0	0
Do	0	8.7	0	5.6	5.4	0	98.3	458.1	0	0	0	0	0
Dc	0	0	0	0	0	0	0	12.2	2.5	0	0	0	0
Eo	0	0	0	0	0	0	15.3	83.3	5.3	204.3	0	0	0
Ec	0	0	0	0	0	0	0	0	0	0	0	0	0
Ft	0	0	0	3	0	0	12.3	79.1	0	189.8	0	847.2	0
Fi	0	0	0	0	0	0	0	0	0	0	0	78.5	93.6

Table 7. Co-occurrence matrix between the scenario ensemble of models for the distant future climate change period 2071–2100 (top of the table) and the ensemble of historical simulations (1961–1990, left). Values are in thousands of square kilometers

	BW	*BS*	*Aw*	*Cs*	*Cw*	*Ar*	*Cr*	*Do*	*Dc*	*Eo*	*Ec*	*Ft*	*Fi*
BW	74	5.6	0	0	0	0	0	0	0	0	0	0	0
BS	23.8	90.8	8.8	46.2	0	0	44.4	0	0	0	0	0	0
Aw	12.1	39.5	4583	0	0	43.1	0	0	0	0	0	0	0
Cs	0	0	13.6	46.5	0	0	335.2	0	0	0	0	0	0
Cw	0	0	14.9	0	46.6	21.5	0	0	0	0	0	0	0
Ar	0	0	1203	0	0	5773.3	0	0	0	0	0	0	0
Cr	0	0	713.1	0	21	789.2	1675.2	0	0	0	0	0	0
Do	0	20.3	0	5.6	18.3	0	282.6	249.2	0	0	0	0	0
Dc	0	0	0	0	0	0	0	14.7	0	0	0	0	0
Eo	0	2.9	0	8.6	0	0	23.9	245.8	9.6	17.5	0	0	0
Ec	0	0	0	0	0	0	0	0	0	0	0	0	0
Ft	0	14.2	0	20.4	0	0	156.2	171.1	0	260.6	0	508.8	0
Fi	0	0	0	0	0	0	0	0	0	0	0	164.7	7.3

gains a large area of land (1.1×10^6 km^2 for 2011–2040 and 1.9×10^6 km^2 for 2071–2100) at the expense of climates *Cr* and *Ar*. The areas of these latter 2 climates decrease the most in projections. *Cr* loses 0.73×10^6 km^2 by the end of the century compared to the reference period (1961–1990); *Ar* suffers a big diminution, lower than that of *Cr*. Curiously, the decreased area of *Ar* with respect to the reference period is lower in the period 2071–2100 than in 2011–2040 because the transitions from *Cr* to *Ar* grow faster throughout the 21st century than those from *Ar* to *Aw*. There are also transitions between ice cap (*Fi*), tundra (*Ft*), subarctic oceanic (*Eo*), temperate oceanic (*Do*) and *Cr* climates. These transitions involve much lower extensions and are always to warmer climates. Transitions between *Ft* and *Cr* and between *Cs* and *Cr* are significant in the period 2071–2100 but negligible for 2011–2041.

Climate transitions in which climate *Cr* (subtropical humid) is involved represent 31.8% of all transitions for the period 2011–2040 relative to the reference period and 47.9% for the period 2071–2100. Virtually all transitions (96.6% for 2011–2040 and 96.2% for 2071–2100) in which a new tropical climate appears where it did not exist in the reference period in any of its 2 forms (*Ar* and *Aw*) depart from climate *Cr*.

Some transitions are especially strong, such as those that occur between *Ft* (tundra) and *Do* (temperate oceanic) or even between *Ft* and *Cr* (subtropical humid). The latter are almost nonexistent for the period 2011–2040 but are significant (1.56×10^5 km^2) for the period 2071–2100.

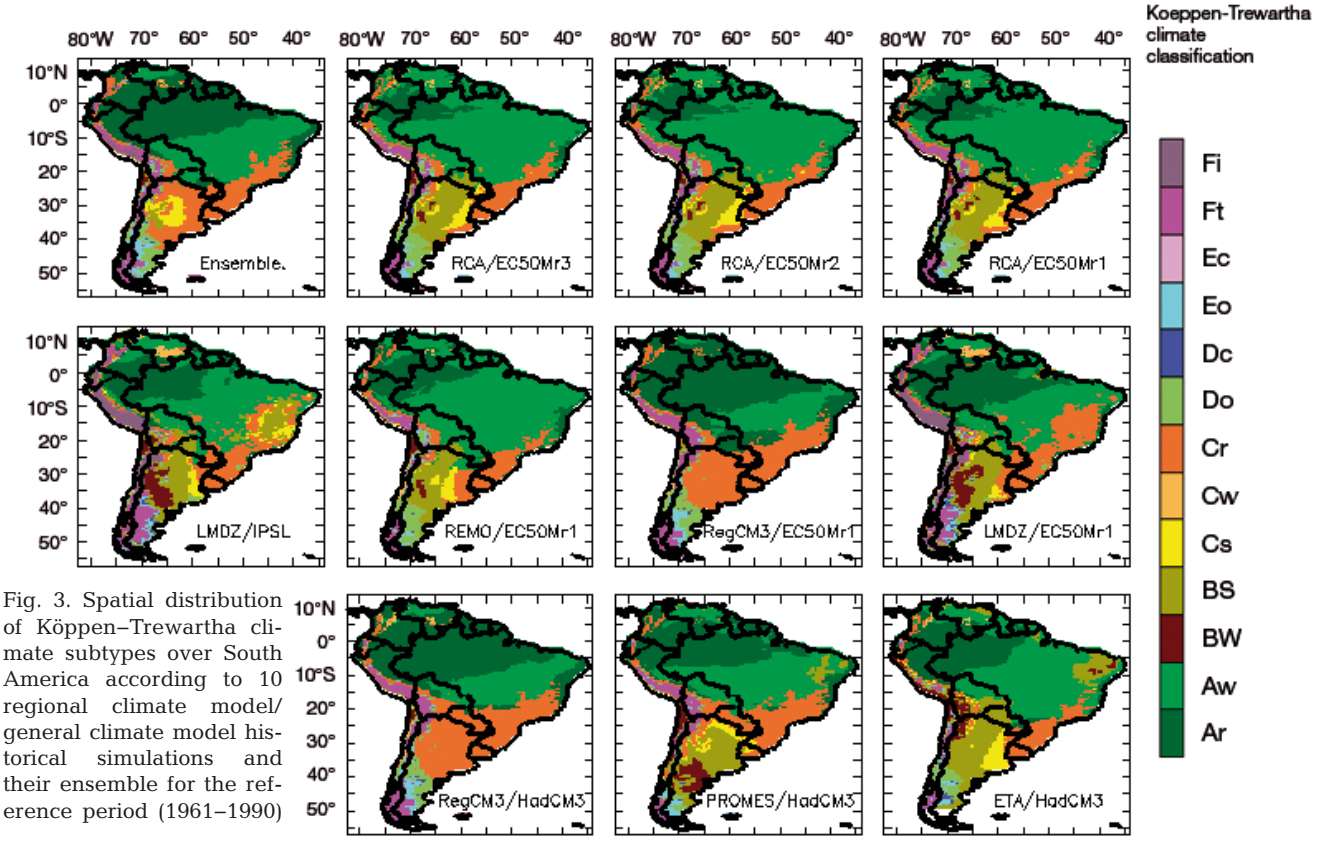

Fig. 3. Spatial distribution of Köppen–Trewartha climate subtypes over South America according to 10 regional climate model/general climate model historical simulations and their ensemble for the reference period (1961–1990)

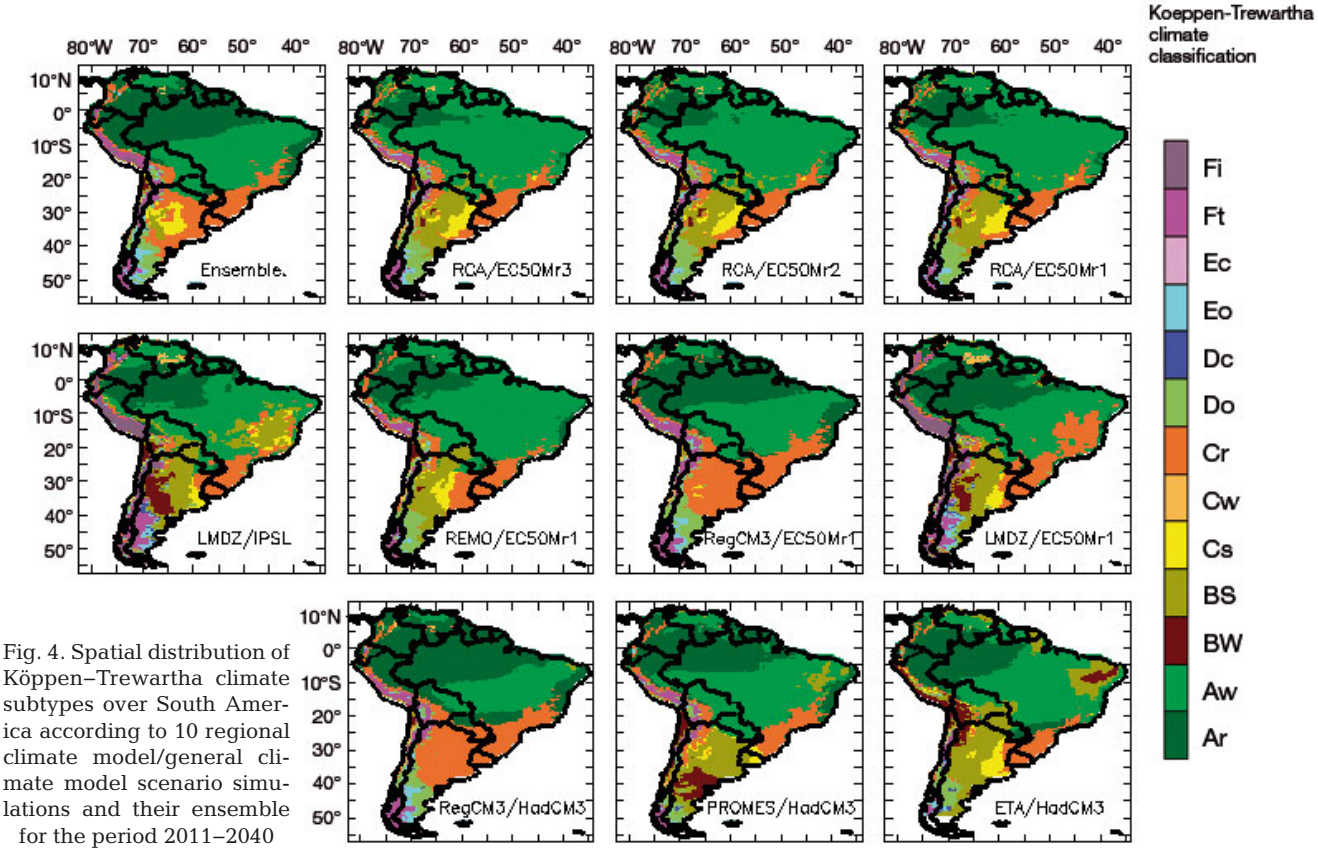

Fig. 4. Spatial distribution of Köppen–Trewartha climate subtypes over South America according to 10 regional climate model/general climate model scenario simulations and their ensemble for the period 2011–2040

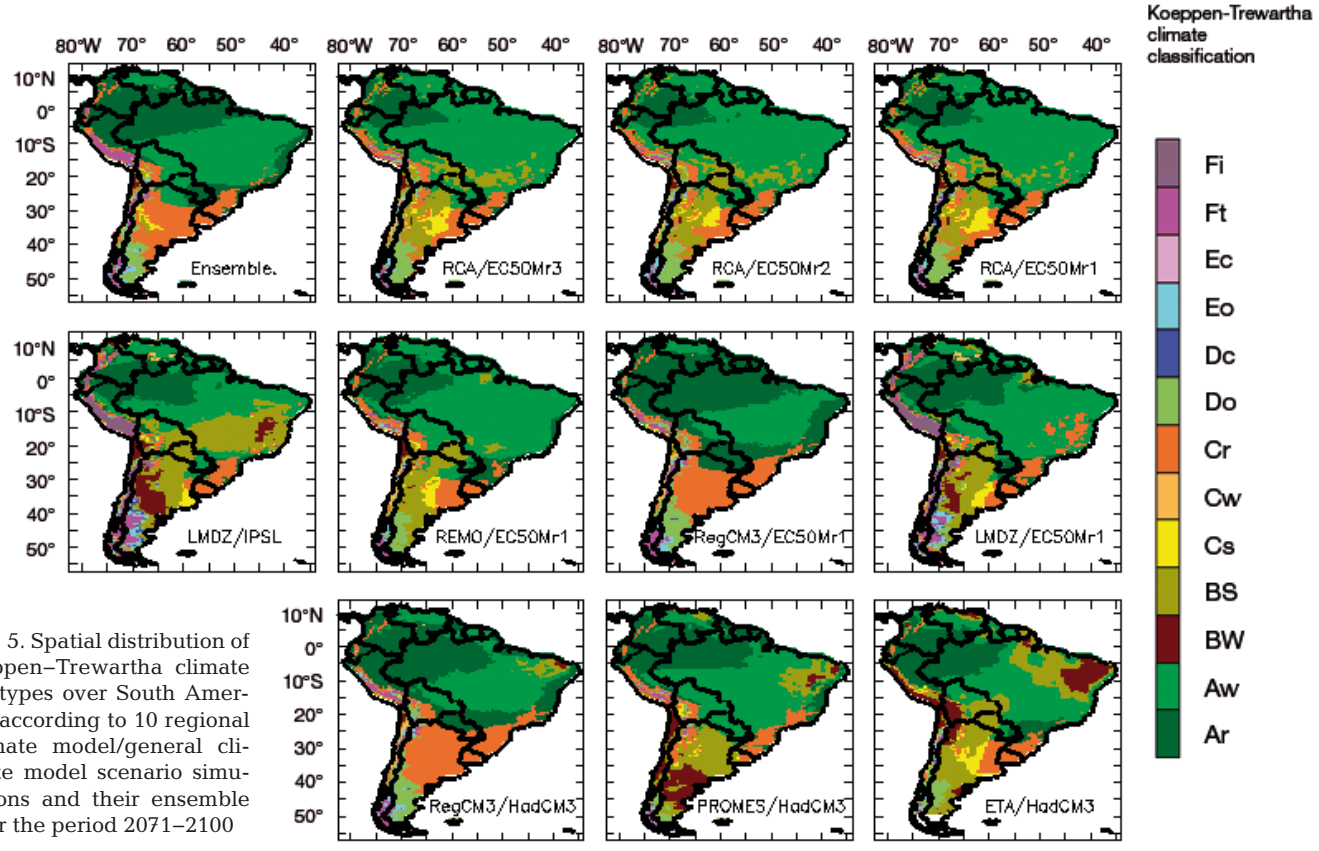

Fig. 5. Spatial distribution of Köppen–Trewartha climate subtypes over South America according to 10 regional climate model/general climate model scenario simulations and their ensemble for the period 2071–2100

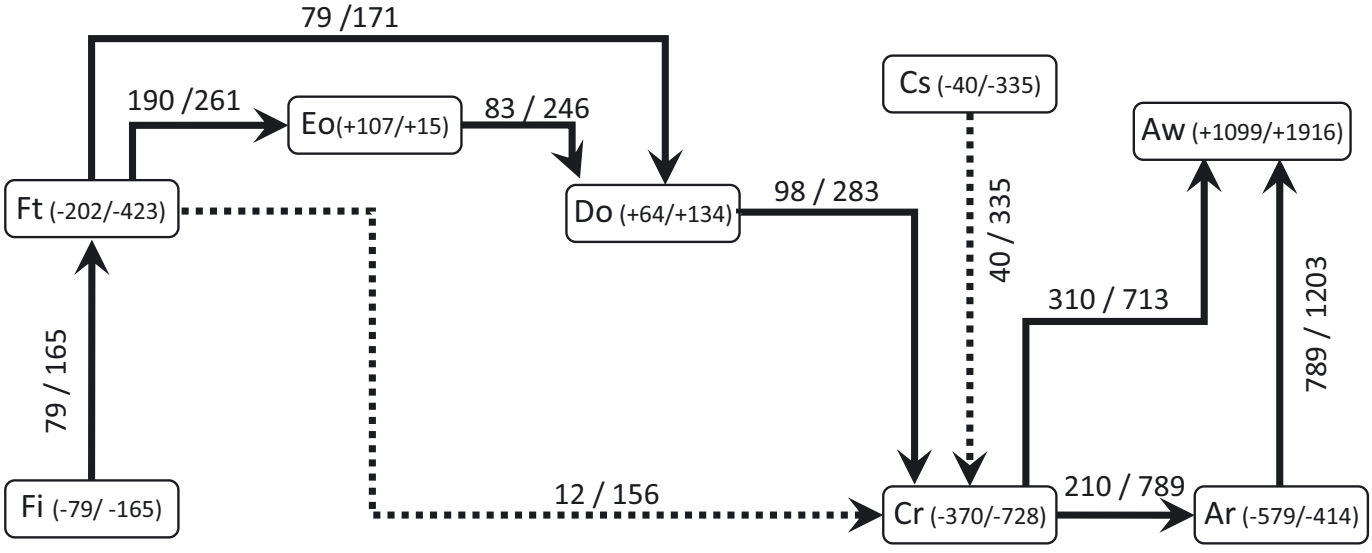

Fig. 6. Transfers between the different Köppen–Trewartha climate subtypes with respect to the reference period 1961–1990 (solid arrows). + or – signs (in parentheses): net gain or loss of area, respectively. Numbers on arrows: net area (10^3 km^2) that undergoes the given transition. Numbers separated by solidus: 2011–2040/2071–2100. Dashed arrows: transfers that are significant for the period 2071–2100 but not for the period 2011–2040

4. CONCLUSIONS

The climate classification of KT has been used to assess simulations over SA performed by 7 RCMs nested in ERA-Interim reanalysis. KT allows us to analyse in an integrated way the results of precipitation and t2m. The results indicate that the ensemble of models represents the climates of SA well enough because it agrees with the observations in 70% of the continental area. This percentage of hits is high when you consider the wide variety and spatial complexity of the climates of SA and the scarcity of reliable observations in many parts of the domain. Moreover, the coincidence between KT climates of individual models and observations ranges from 48 to 67%. A similar study, focused over Europe (Gallardo et al. 2013), showed higher values, 83.5% for the ensemble of models and a range from 55.4 to 81.3% for individual models. These differences could be partly due to the coarser resolution used here (50 km compared to 25 km over Europe). Another factor that could explain the differences is the smaller amount of observational data used to construct the CRU database over SA compared with the amount used over Europe (New et al. 2002) and, therefore, the larger uncertainty in those observations to correctly represent regional climates. Besides that, Solman et al. (2013) indicated that despite the main seasonal and observational features reasonably described by the RCMs over SA, some systematic biases were also obtained over certain subregions and periods and that these biases are not generally obtained for regional simulations over Europe (e.g. Jacob et al. 2007, Kjellström et al. 2010). This is particularly noticeable for the underestimation of precipitation over southeastern Brazil and Uruguay in the austral winter. The variety of climates and orographic complexity over SA are greater than they are over Europe, and are additional factors that could help to explain such differences between the continents. Moreover, as in other works over other regions, it is also true that the ensemble provides better results than any of the individual models.

For historical simulations, the level of coincidence with the observed KT climates ranges from 52.0 to 65.2%. According to Gallardo et al. (2013), almost equivalent simulations for Europe gave percentages of agreement with observations between 65.3 and 81.3%, that is, about 15 percentage points less. The arguments given in the previous paragraph to justify a worse performance of hindcast simulations in SA than in Europe are also valid here. Furthermore, it is known that GCMs do not resolve the climate well in some parts of SA, especially in the steep eastern coast of this region (Flato et al. 2013).

Ten RCM simulations for the SRES A1B scenario over SA have also been analysed to study how the KT climates are projected to change due to increased greenhouse gas conditions. Transitions to wetter climates are found in small areas of the domain that represent up to 3% of the area of SA for the period 2071–2100. Most of these changes are detected in the northern half of Argentina. Transitions to drier or warmer climates are also projected, occurring in 24% of the territory of SA for the period 2071–2100 and in 11.5% for the nearer future (2011–2040). Therefore, changes in KT climate are projected over a considerable portion of SA. In this study, it is projected that about 12% of the area of SA will be affected by significant climate changes for the period 2011–2040 and around 27% for 2071–2100. But even more important is that these results indicate that these changes in climate have been occurring at an appreciable pace since the beginning of the 21st century. According to this result, studies in which climate change is detected in SA should become increasingly numerous in the coming years.

Some of the climate transitions projected in this study are very strong, especially those from *Ft* (tundra) to *Do* (temperate oceanic) and from *Ft* to *Cr* (subtropical humid). These large changes are projected to start in a few decades at points throughout the mountain range of the Andes, and they may be associated with strong stresses on ecosystems and hydrological systems in these areas. Some of these details indicate the nonlinearity of the evolution of climate change over the 21st century.

The climate *Cr* appears in a large number of climate transitions. It is the origin of almost all transitions to new tropical climates. Moreover, transitions involving nontropical climates tend to converge in climate *Cr*. The *Cr* climate seems to be the pivot point for the entire system of transitions between climates projected for SA. This therefore suggests that the study of the subtropical humid climate should be a priority for understanding climate change in this region.

Acknowledgements. We thank the CLARIS-LPB EU-FP7 project (proposal 212492) for providing the results of its simulations for this study. This work was partially funded by the Spanish Ministry of Education and Science and the European Regional Development Fund through grants CGL2007-66440-C04-02 and CGL2010-18013. It was also partially funded by the Spanish Ministry of Economy and Competitiveness through grant CGL2013-47261-R. We acknowledge the Climate Research Unit from the University

of East Anglia for facilitating its observational data. The remarks and suggestions from 3 anonymous reviewers helped to improve the manuscript.

LITERATURE CITED

Antic S, Laprise R, Denis B, de Elía R (2006) Testing the downscaling ability of a one-way nested regional climate model in regions of complex topography. Clim Dyn 26: 305–325

Baker B, Diaz H, Hargrove W, Hoffman F (2010) Use of the Köppen–Trewartha climate classification to evaluate climatic refugia in statistically derived ecoregions for the People's Republic of China. Clim Change 98:113–131

Chou SC, Marengo JA, Lyra A, Sueiro G and others (2012) Downscaling of South America present climate driven by 4-member HadCM3 runs. Clim Dyn 38:635–653

Christensen JH, Carter TR, Rummukainen M, Amanatidis G (2007) Evaluating the performance and utility of regional climate models: the PRUDENCE project. Clim Change 81:1–6

da Rocha RP, Morales CA, Cuadra SV, Ambrizzi T (2009) Precipitation diurnal cycle and summer climatology assessment over South America: an evaluation of regional climate model version 3 simulations. J Geophys Res 114:D10108, doi:10.1029/2008JD010212

de Castro M, Gallardo C, Jylha K, Tuomenvirta H (2007) The use of climate-type classification for assessing climate change effects in Europe from an ensemble of nine regional climate models. Clim Change 81:329–341

Dee DP, Uppala SM, Simmons AJ, Berrisford P and others (2011) The ERA Interim reanalysis: configuration and performance of the data assimilation system. QJR Meteorol Soc 137:553–597

Dimitrijevic M, Laprise R (2005) Validation of the nesting technique in a regional climate model and sensitivity tests to the resolution of the lateral boundary conditions during summer. Clim Dyn 25:555–580

Domínguez M, Gaertner MA, de Rosnay P, Losada T (2010) A regional climate model simulation over West Africa: parameterization tests and analysis of land-surface fields. Clim Dyn 35:249–265

Feser F (2006) Enhanced detectability of added value in limited-area model results into different spatial scales. Mon Weather Rev 134:2180–2190

Flato G, Marotzke J, Abiodun B, Braconnot P and others (2013) Evaluation of climate models. In: Stocker TF, Qin DH, Plattner GK, Tignor M and others (eds) Climate change 2013: the physical science basis. Contribution of Working Group I to the Fifth Assessment Report of the Intergovernmental Panel on Climate Change. Cambridge University Press, Cambridge, p 810–815

Gallardo C, Gil V, Hagel E, Tejeda C, de Castro M (2013) Assessment of climate change in Europe from an ensemble of regional climate models by the use of Köppen–Trewartha classification. Int J Climatol 33:2157–2166

Gao X, Giorgi F (2008) Increased aridity in the Mediterranean region under greenhouse gas forcing estimated from high resolution simulations with a regional climate model. Global Planet Change 62:195–209

Garreaud RD, Vuille M, Compagnucci R, Marengo J (2009) Present-day South American climate. Palaeogeogr Palaeoclimatol Palaeoecol 281:180–195

Giorgi F, Jones C, Asrar GR (2009) Addressing climate information needs at the regional level: the CORDEX framework. WMO Bull 58:175–183

Grell GA, Dudhia J, Stauffer DR (1994) A description of the fifth generation Penn System/NCAR mesoscale model (MM5). NCAR Tech Note NCAR/TN-398+STR, National Center for Atmospheric Research, Boulder, CO

Hourdin F, Musat I, Bony S, Braconnot P and others (2006) The LMDZ4 general circulation model: climate performance and sensitivity to parameterized physics with emphasis on tropical convection. Clim Dyn 27:787–813

Jacob D, Van den Hurk BJJM, Andrae U, Elgered G and others (2001) A comprehensive model intercomparison study investigating the water budget during the BALTEX-PIDCAP period. Meteorol Atmos Phys 77: 19–43

Jacob D, Bärring L, Christensen OB, Christensen JH and others (2007) An inter-comparison of regional climate models for Europe: model performance in present-day climate. Clim Change 81:31–52

Jacob D, Elizalde A, Haensler A, Hagemann S and others (2012) Assessing the transferability of the regional climate model REMO to different COordinated Regional Climate Downscaling EXperiment (CORDEX) regions. Atmosphere 3:181–199

Kjellström E, Boberg F, Castro M, Christensen JH, Nikulin G, Sanchez E (2010) Daily and monthly temperature and precipitation statistics as performance indicators for regional climate models. Clim Res 44:135–150

Laprise R (2008) Regional climate modelling. J Comput Phys 227:3641–3666

Li L (1999) Ensemble atmospheric GCM simulation of climate interannual variability from 1979 to 1994. J Clim 12: 986–1001

Matsuura K, Willmott CJ (2009) Terrestrial air temperature: 1900–2008 gridded monthly time series (version 2.01). Center for Climatic Research, Department of Geography, University of Delaware, Newark. http://climate.geog.udel.edu/~climate/

Mitchell TD, Jones PD (2005) An improved method of constructing a database of monthly climate observations and associated high-resolution grids. Int J Climatol 25: 693–712

Nakićenović N, Alcamo J, Davis G, de Vries B and others (2000) Special report on emissions scenarios. Special report of Working Group III of the Intergovernmental Panel on Climate Change. Cambridge University Press, Cambridge

New M, Lister D, Hulme M, Makin I (2002) A high-resolution data set of surface climate over global land areas. Clim Res 21:1–25

Pal JS, Giorgi F, Bi X, Elguindi N and others (2007) The ITCP RegCM3 and RegCNET: regional climate modeling for the developing World. Bull Am Meteorol Soc 88: 1395–1409

Pesquero JF, Chou SC, Nobre CA, Marengo JA (2010) Climate downscaling over South America for 1961–1970 using the Eta model. Theor Appl Climatol 99:75–93

Rauscher S, Coppola E, Piani C, Giorgi F (2010) Resolution effects on regional climate model simulations of seasonal precipitation over Europe. Clim Dyn 35:685–711

Roderfeld H, Blyth E, Dankers R, Huse G and others (2008) Potential impact of climate change on ecosystems in the Barents Sea region. Clim Change 87:283–303

Samuelsson P, Kourzeneva E, Mironov D (2010) The impact of lakes on the European climate as simulated by a

regional climate model. Boreal Environ Res 15:113–129

Samuelsson P, Jones CG, Willén U, Ullerstig A and others (2011) The Rossby Centre regional climate model RCA3: model description and performance. Tellus A Dyn Meteorol Oceanogr 63:4–23

Samuelsson P, Solman S, Sánchez E, Rocha R and others (2013) Regional climate change projections over South America based on the CLARIS-LPB RCM ensemble. Geophys Res Abstr 15:EGU2013-5800

Sánchez E, Gaertner MA, Gallardo C, Padorno E, Arribas A, Castro M (2007) Impacts of change in vegetation description on simulated European summer present-day and future climates. Clim Dyn 29:319–332

Sánchez E, Solman S, Berbery H, Samuelsson P and others (2011) A first look at an ensemble of XXIst century RCM simulations over South America. WCRP Open Science Conference, 24–28 Oct 2011, Denver, CO

Sánchez E, Solman S, Remedio ARC, Berbery H and others (2015) Regional climate modelling in CLARIS-LPB: a concerted approach towards twenty-first century projections of regional temperature and precipitation over South America. Clim Dyn, doi:10.1007/s00382-014-2466-0

Shi Y, Gao XJ, Wu J (2012) Projected changes in Köppen climate types in the 21st century over China. Atmos Oceanic Sci Lett 5:495–498

Simmons AJ, Uppala SM, Dee DP, Kobayashi S (2007) ERA-Interim: new ECMWF reanalysis products from 1989 onwards. ECMWF Newsl 110:25–35

Solman S, Pessacg N (2012) Regional climate simulations over South America: sensitivity to model physics and to the treatment of lateral boundary conditions using the MM5 model. Clim Dyn 38:281–300

Solman SA, Sánchez E, Samuelsson P, da Rocha RP and others (2013) Evaluation of an ensemble of regional climate model simulations over South America driven by the ERA-Interim reanalysis: model performance and uncertainties. Clim Dyn 41:1139–1157

Trewartha GT, Horn LH (1980) An introduction to climate, 5th edn. McGraw-Hill, New York, NY

Urrutia R, Vuille M (2009) Climate change projections for the tropical Andes using a regional climate model: temperature and precipitation simulations for the end of the 21st century. J Geophys Res 114:D02108, doi:10.1029/2008JD011021

Vera C, Baez J, Douglas M, Emmanuel CB and others (2006a) The South American low-level jet experiment. Bull Am Meteorol Soc 87:63–77

Vera C, Higgins W, Amador J, Ambrizzi T and others (2006b) Toward a unified view of the American monsoon systems. J Clim 19:4977–5000

Vera C, Silvestri G, Liebmann B, González P (2006c) Climate change scenarios for seasonal precipitation in South America from IPCC-AR4 models. Geophys Res Lett 33: L13707, doi:10.1029/2006GL025759

Editorial responsibility: Andrea Carril (Guest Editor), Buenos Aires, Argentina

Submitted: September 22, 2014; Accepted: August 22, 2015
Proofs received from author(s): December 3, 2015